NASA Technical Memorandum 108989

NASA-TM-108989 19940033125

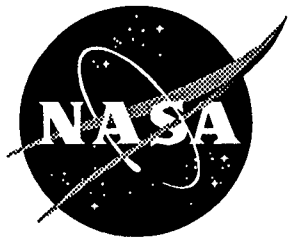

Stability Analysis of an F/A-18 E/F Cable Mount Model

Nancy Thompson and Moses Farmer
Langley Research Center, Hampton, Virginia

June 1994

National Aeronautics and
Space Administration
Langley Research Center
Hampton, Virginia 23681-0001

STABILITY ANALYSIS OF AN F/A-18 E/F CABLE MOUNT MODEL

Nancy Thompson and Moses Farmer

SUMMARY

A full-span F/A-18 E/F cable mounted wind-tunnel model is part of a flutter clearance program at the NASA Langley Transonic Dynamics Tunnel. Parametric analysis of this model using GRUMCBL software was conducted to assess stability for wind-tunnel tests. Two configurations of the F/A-18 E/F were examined. The parameters examined were pulley-cable friction, Mach number, dynamic pressure, cable geometry, center of gravity location, cable tension, snubbing the model, drag, and test medium. For the nominal cable geometry (Cable Geometry 1), Configuration One was unstable for cases with higher pulley-cable friction coefficients. A new cable geometry (Cable Geometry 3) was determined in which Configuration One was stable for all cases evaluated. Configuration Two with the nominal center of gravity position was found to be unstable for cases with higher pulley-cable friction coefficients; however, the model was stable when the center of gravity was moved forward 1/2 inch. The model was tested using the cable mount system during the initial wind-tunnel entry and was stable as predicted.

INTRODUCTION

A full-span F/A-18 E/F wind-tunnel model is part of a flutter clearance program at the NASA Langley Transonic Dynamics Tunnel (TDT)[1]. The F/A-18 E/F is a modification of the existing F/A-18 C/D aircraft. Modifications include added capability in terms of range and payload, increased size of all surfaces, and a 34 inch fuselage extension. Since flutter instabilities on an aircraft may involve interaction between elastic and rigid-body modes, the two-cable mount system is being used to permit simulation of the free-flight rigid-body modes[2]. Previous flutter clearance tests using cable mounted models include the F-14, F-15, F-16, F-16XL, and F-111. Previous research studies which used cable mounted wind-tunnel models include gust loads studies conducted in 1966 with the F-106 wind-tunnel model[3] and in 1979 with the B-52E wind-tunnel model[4], and an airplane aileron effectiveness study conducted using the C-141 wind-tunnel model[5]. Also, a nacelle aerodynamic effects study was conducted using the low-speed 747 wind-tunnel model[6] and an active wing/store flutter suppression study was conducted using the F-16 flutter suppression model[7].

This report summarizes a stability study conducted on the F/A-18 E/F cable mount model prior to wind-tunnel testing. The purpose of this study was to examine the effect of various model, mount system, and tunnel parameters on rigid model stability. The parameters examined were flow-conditions (Mach number and dynamic pressure), pulley-cable friction, cable geometry, center of gravity location, cable tension, snubber effects, drag, and test medium. A significant amount of pulley-cable friction exists which can adversely affect longitudinal stability of the model. Since pulley-cable friction is not well-modeled, some of the parameter studies were repeated over a range of pulley-cable friction coefficients. Since most of the wind-tunnel tests were to be conducted with R-12 as the test medium, the majority of this study used velocities and flow densities appropriate for R-12. Stability of the model using velocities and flow densities appropriate for air was also examined briefly since initial wind-tunnel tests were to be conducted in air. The model was

tested using the cable mount configuration during the first wind-tunnel entry and was stable as predicted. The wind-tunnel test will not be discussed since frequency and damping of the rigid-body modes were not measured.

SYMBOLS

BL	tunnel butt line, in.
C_D	drag coefficient
C_{D_M}	model drag coefficient
C_{D_S}	effective snubber drag coefficient
c.g.	center of gravity, in.
Cmp	pulley-cable friction coefficient, ft-lbs/rad/sec
Cmpf	forward pulley-cable friction coefficient, ft-lbs/rad/sec
Cmpr	rear pulley-cable friction coefficient, ft-lbs/rad/sec
d_{sc}	snubber cable diameter, in.
D_S	snubber cable damping coefficient, lb-sec/in
f	frequency, Hz
FS	fuselage station, in.
h	total pressure, psf
K_S	snubber cable spring constant, lb/in
l_{sc}	length of snubber cable, in.
M	Mach number
q	dynamic pressure, psf
S_M	wing area, ft^2
S_S	effective snubber surface area, ft^2
T_R	rear cable tension, lbs.
TS	tunnel station, in.
T_S	snubber cable tension, lbs.
ζ	damping ratio of model
WL	tunnel water line, in.

ANALYTICAL AND TEST MODEL

The F/A-18 E/F wind-tunnel model is an 18 percent full-span model with rigid and flexible surfaces available for testing. The model can be tested on a sting or on a cable mount. All rigid surfaces were used for the initial cable mount test to determine stability of the free-flight rigid body modes. A picture of the cable mounted model in the TDT is shown in Figure 1. The model is 10.8 ft. in length and has a 7.5 ft. wing span. The "flying-model" cable configuration consisted of horizontally-oriented forward cables and vertically-oriented rear cables. The cables were kept under tension by stretching a soft spring in the rear cables. A "snubber cable" system was also used. The snubber cable system consists of four cables, normally slack during testing, which can be remotely activated to snub or restrain the model in case an instability occurs.

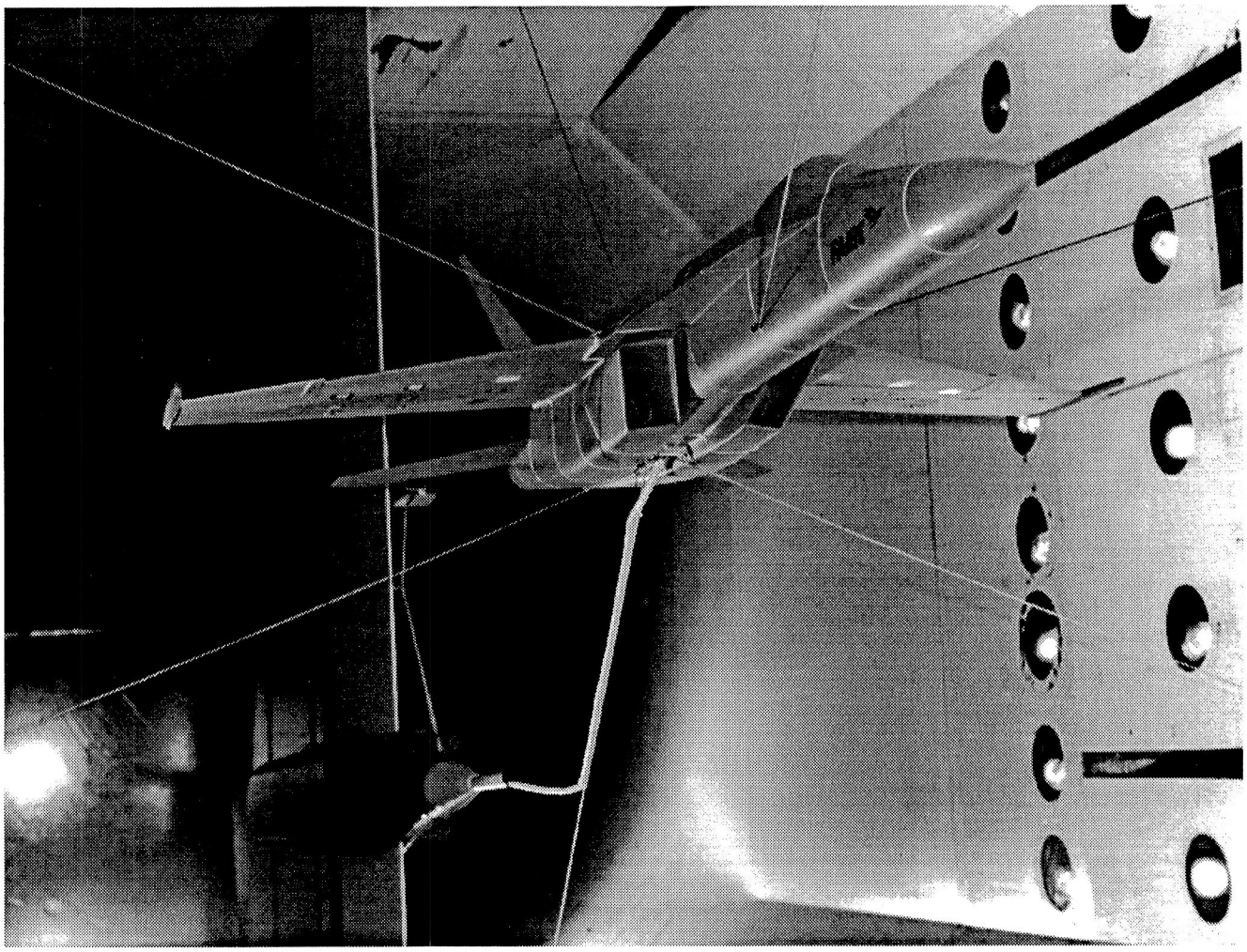

Figure 1. The F/A-18 E/F rigid model cable mounted in the NASA Langley Transonic Dynamics Tunnel

Two analytical models of the F/A-18 E/F model were examined in this stability analysis. Configuration One represented the test configuration with the heaviest weight and Configuration Two represented the test configuration with the lightest weight. The c.g. locations of both configurations were variable. The nominal c.g. locations were FS 83.6 for Configuration One and FS 87.9 for Configuration Two. The wind-tunnel model as tested fell between these two analytical cases in terms of both weight and c.g. positions. The aerodynamic coefficients and stability derivatives for Configuration One as specified for the analysis routine are listed in Table 1.

Three cable geometries were analyzed to find the effect of cable geometry on rigid body stability. The forward and rear cable tie-down positions for Cable Geometry 1 were located at TS 588 and TS 912, respectively. For Cable Geometry 2, the rear cable tie-down position was moved further aft 48 inches to TS 960, and the forward tie-down position remained at TS 588. For Cable Geometry 3, the forward cable was moved forward 72 inches to TS 516, and the rear cable tie-down position remained at TS 960. Cable Geometry 3 was selected for the wind-tunnel test and is illustrated in Figure 2.

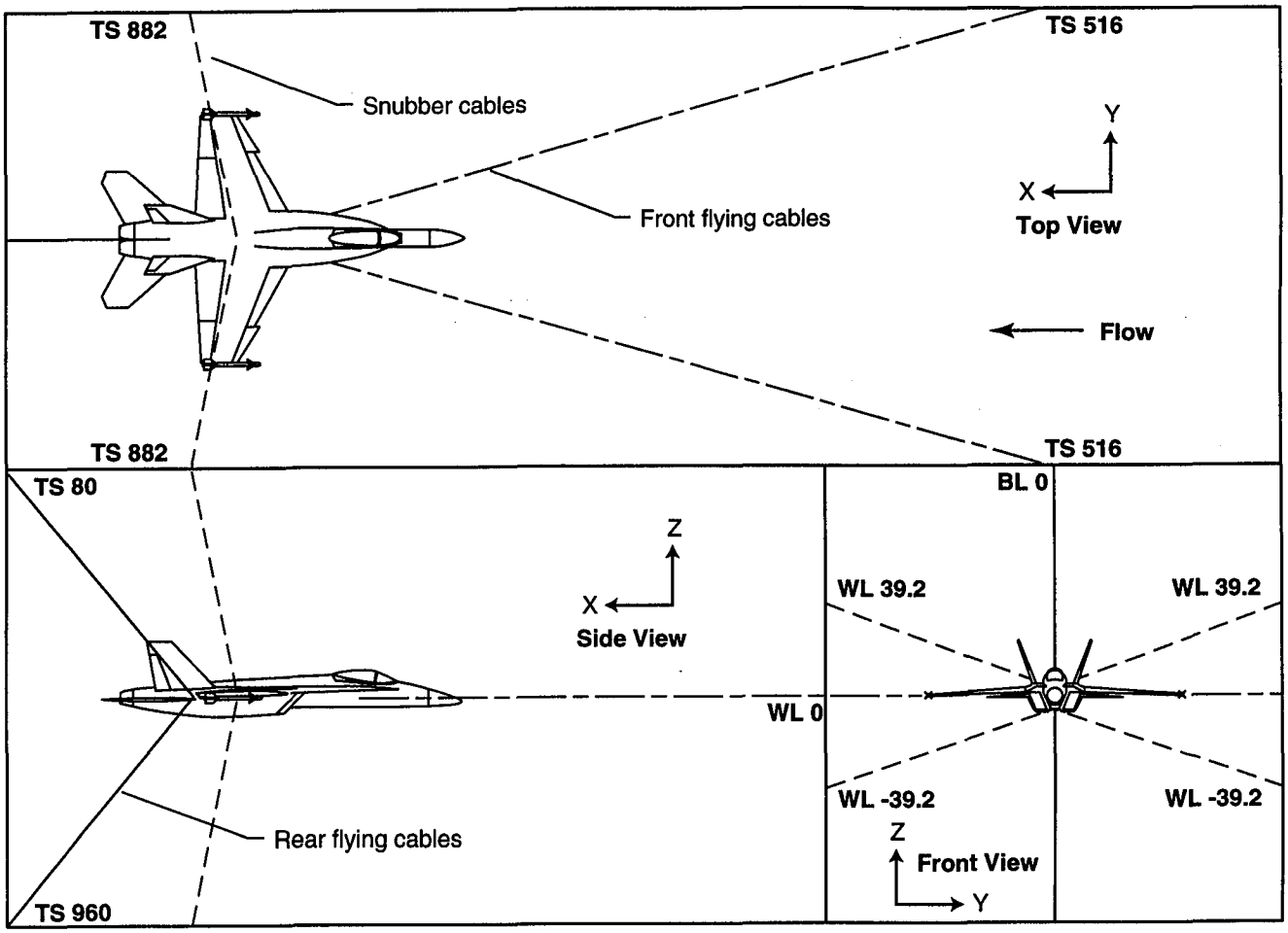

Figure 2. Cable Geometry 3 for the F/A-18 E/F model.

ANALYTICAL TOOLS

A computer program developed to analyze the rigid body stability of cable mounted models in the TDT, known as GRUMCBL[8], was used for this analytical study. With this software, various model, tunnel, and cable system parameters can be varied independently to analyze their affect on rigid model stability. GRUMCBL calculates the forces and moments due to vehicle weight, aerodynamics, and cables, and solves linearized equations of motion. There are two longitudinal modes: vertical translation and short period; and three lateral modes: side translation, a heavily damped roll-yaw mode, and dutch roll. The vertical translation mode was the critical mode with respect to rigid model stability for all of the cases analyzed, so this report will concentrate on how the various parameters affected this mode.

Configuration One was used primarily throughout this study, thus the majority of the results in this report are for this configuration. The effect of the following model, tunnel, and cable system parameters on rigid-body stability of Configuration One was examined: pulley-cable friction, Mach number, dynamic pressure, cable geometry, c.g. position, rear cable tension, snubber cable system, model and cable drag, and air as the test medium. Three cable configurations, Cable Geometry 1, 2 and 3, were studied with the objective of finding the most stable configuration. Some of the analyses conducted on Configuration One were repeated using Configuration Two with the purpose of determining whether or not the rigid-body modes followed the same trends as parameters were varied as was found

with Configuration One. Since the trends were found to be similar, only the results of the c.g. position study will be reported for Configuration Two.

All input data pertaining to the model, mount systems, tunnel conditions, and aerodynamic performance are defined in an array called AERO. The AERO array number and other pertinent information are listed as each parameter is discussed in this report. Input data for Configuration One at M = 0.7 and M = 1.2 using Cable Geometry 3 are listed in Table 1. An example of an output listing from GRUMCBL analysis is shown in the Appendix.

RESULTS AND DISCUSSION

Pulley-Cable Friction Effects

Pulley-cable friction is known to have a significant effect on stability and a range of pulley-cable friction coefficients (Cmp) were used throughout this analysis. For GRUMCBL analysis, the rear pulley-cable friction coefficient (Cmpr) and forward pulley-cable friction coefficient(Cmpf) are input as AERO(104) and AERO(126) respectively. In this study, Cmpr and Cmpf were always set equal to each other, and will subsequently be referred to as Cmp. The range for Cmp was determined by a "wind-off" analysis of Configuration One. Previous wind-tunnel experience with cable-mounted models showed that in the wind-off condition, the vertical translation damping ratio of the model was between 0.1 and 1.0. Various values of Cmp were used in the analysis to find coefficients which produced damping ratios between 0.1 and 1.0 for the vertical translation mode. Cmp values which produced the desired damping ratios were between .02 and .08.

Stability analyses were conducted on Configuration One using Cable Geometry 1, with Cmp ranging from 0.0 to .08, at the following flow conditions in R-12: M=0.7 and q=75 psf, M=0.7 and q=150 psf, M=1.2 and q=150 psf, and M=1.2 and q=300 psf. With Cable Geometry 1, the front cables were attached to the tunnel walls at Tunnel Station (TS) 588 (AERO(72)), and the rear cables were attached to the tunnel ceiling and floor at TS 912 (AERO(73)). The resulting frequencies and damping ratios for each mode are plotted in Figures 3a through 3e.

Cmp had a significant effect on rigid body damping, especially on the vertical translation mode (Figure 3a). At M=0.7, the damping ratio of the vertical translation mode decreased significantly as Cmp was increased. At M=0.7 and q=150 psf, the mode became unstable at Cmp=.04 and higher. At M=0.7 and q=75 psf, the mode became unstable at Cmp=.06 and higher. Cmp had the opposite effect on vertical translation damping at M=1.2. Damping increased as Cmp was increased.

The short period mode and lateral translation mode were beneficially affected by Cmp. As shown in Figures 3b and 3c, the damping ratios of these modes increased as Cmp increased. The roll-yaw, and dutch roll modes were not significantly affected by Cmp (Figures 3d and 3e). Note that for the roll-yaw mode (Figure 3d), there are no frequency or damping ratio curves for M=1.2 and q=300 psf. This is due to the mode converging to two negative real roots at this flow condition; therefore, the frequency was zero and the damping ratio was infinite.

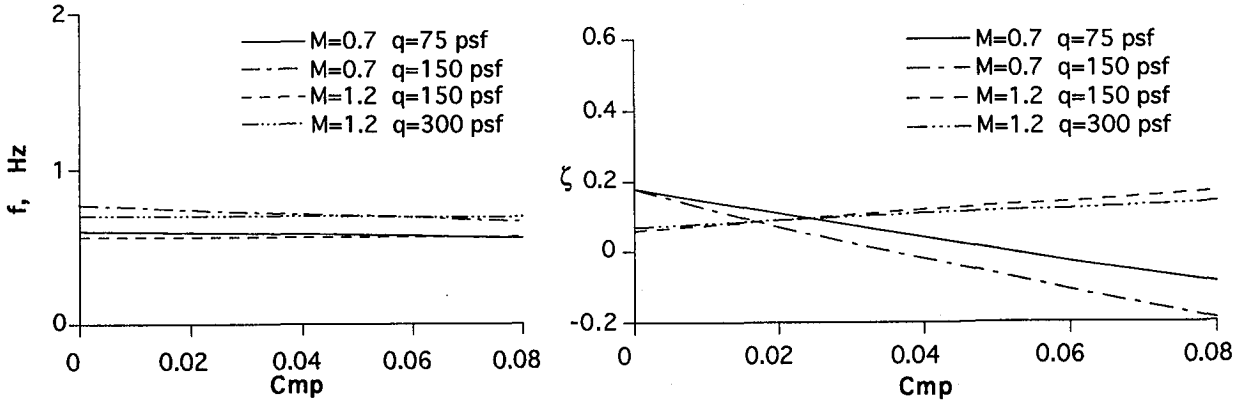

Figure 3(a) Vertical translation

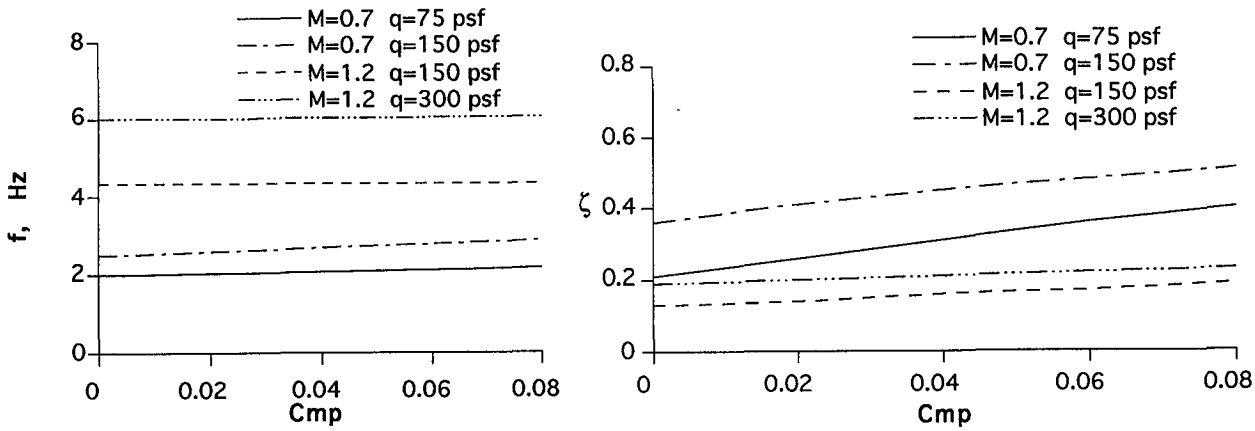

Figure 3(b) Short period

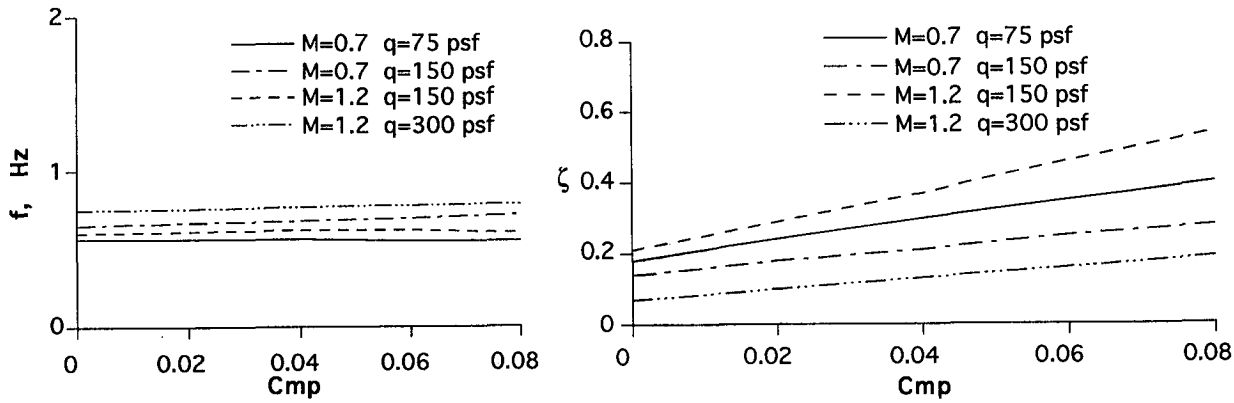

Figure 3(c) Lateral translation

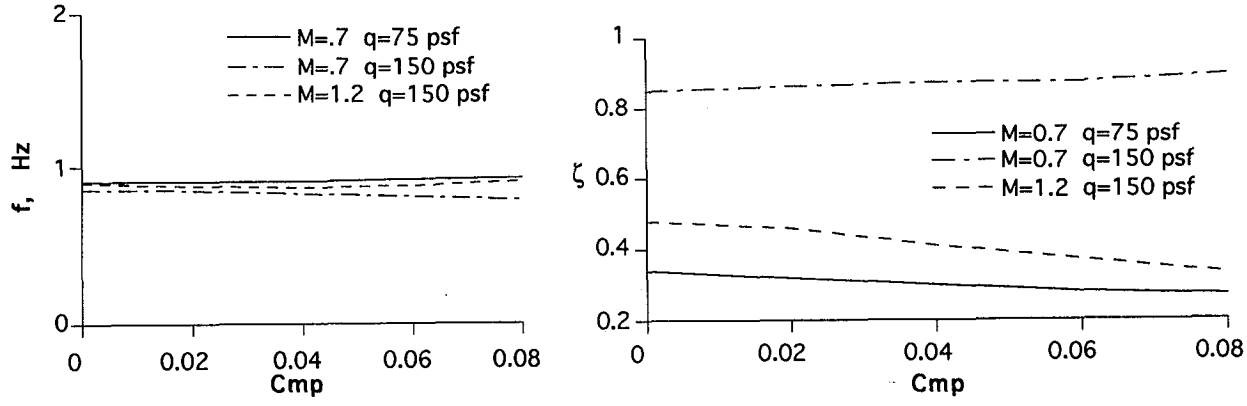

Figure 3(d) Roll-yaw

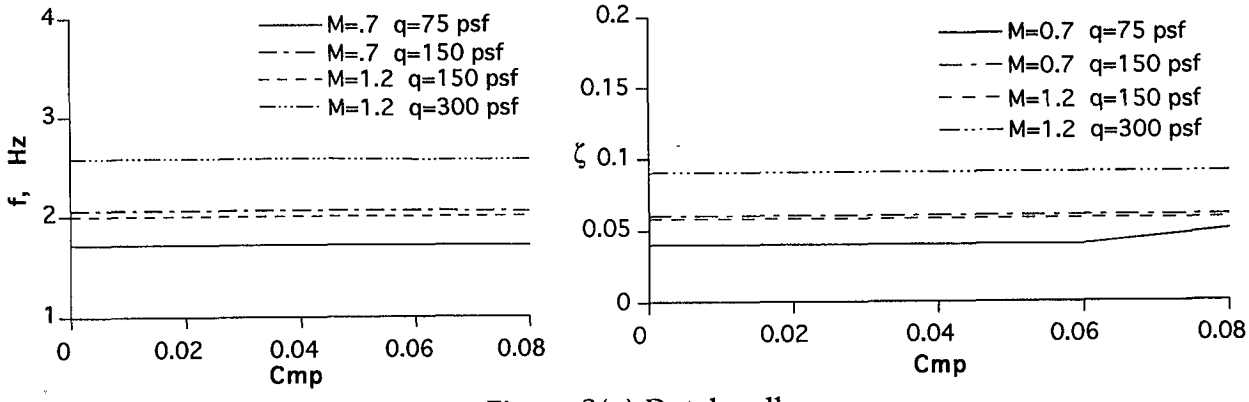

Figure 3(e) Dutch roll

Figure 3. Rigid body modes for Configuration One with respect to pulley-cable friction.

Mach Number And Dynamic Pressure

Stability analyses were conducted on Configuration One, Cable Geometry 1, Cmp=.04 at M=0.7, M=0.9 and M=1.2, and dynamic pressure ranging from 75 psf to 300 psf. The resulting frequency and damping of the five rigid-body modes are shown in Figures 4a-4e.

Although the vertical translation mode frequency (Figure 4a) increased as dynamic pressure increased, at constant dynamic pressure, the frequency decreased as Mach number increased. Damping did not vary significantly with dynamic pressure; however at M=0.7 and M=0.9, the damping ratio decreased enough so that the mode became unstable at q=150 psf. There was a slight increase in the damping ratio as dynamic pressure increased further; however, the mode remained unstable. At constant dynamic pressure, the damping ratio increased as Mach number increased. The increase was the greatest between M=0.9 and M=1.2.

The short period mode frequency (Figure 4b) increased significantly as dynamic pressure increased. The rate of increase was the greatest at M=1.2. At constant dynamic pressure, the frequency increased significantly as Mach number increased. The damping ratio also increased as dynamic pressure increased; however, damping decreased as Mach number increased.

The frequency and damping ratio of the lateral translation mode (Figure 4c) did not vary significantly as dynamic pressure and Mach number were varied. The frequency increased slightly as dynamic pressure increased. At lower dynamic pressure, the frequency decreased slightly as Mach number increased. Except for an initial increase in the damping ratio at M=0.9 and M=1.2, lateral mode damping generally decreased as dynamic pressure increased.

Mach number and dynamic pressure had a significant effect on the roll-yaw mode (Figure 4d). This mode converged to two negative real roots (f=0 Hz) at M=0.7 and q=200 psf, M=0.9 and q=300 psf, and at M=1.2 and q=300 psf. The damping ratio increased significantly as dynamic pressure increased with $\zeta = \infty$ when the mode converged.

The dutch roll mode frequency (Figure 4e) increased as dynamic pressure increased. At constant dynamic pressure, the frequency decreased initially as Mach number increased from 0.7 to 0.9 and then increased as Mach number increased further to 1.2. The damping ratio increased slightly as dynamic pressure increased. At constant dynamic pressure, the damping ratio did not change significantly as Mach number increased.

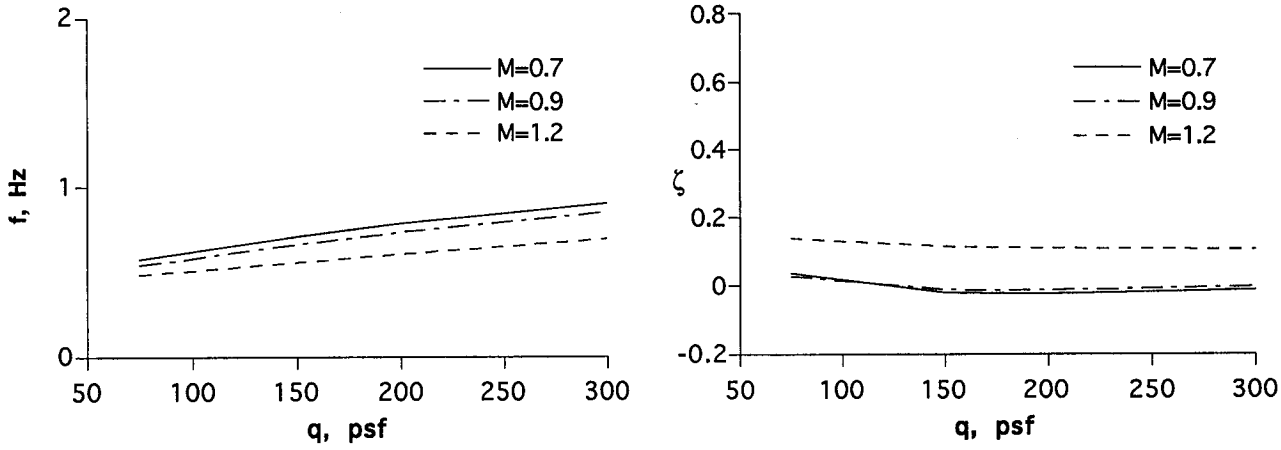

(a) Vertical translation

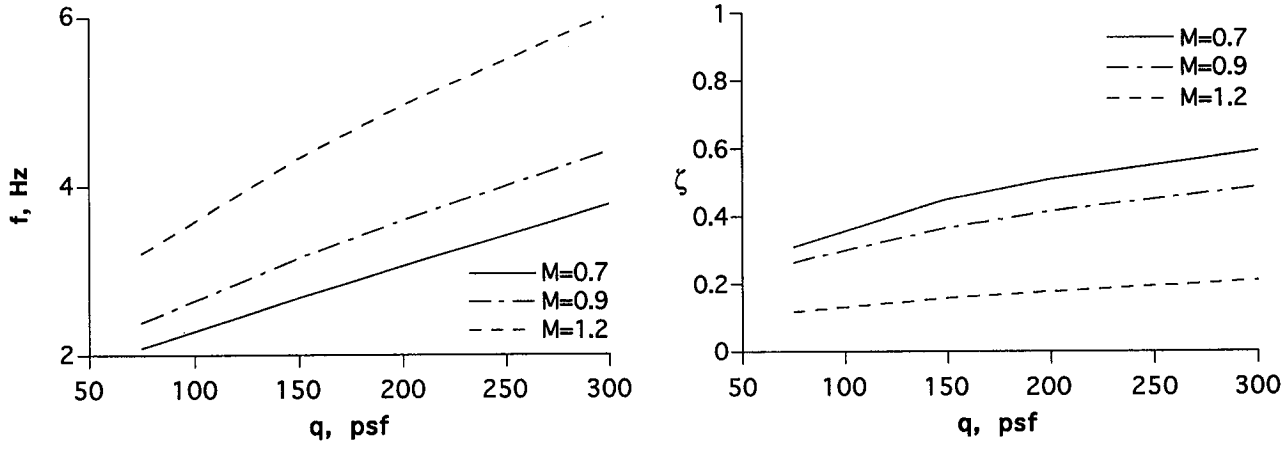

Figure 4(b) Short period

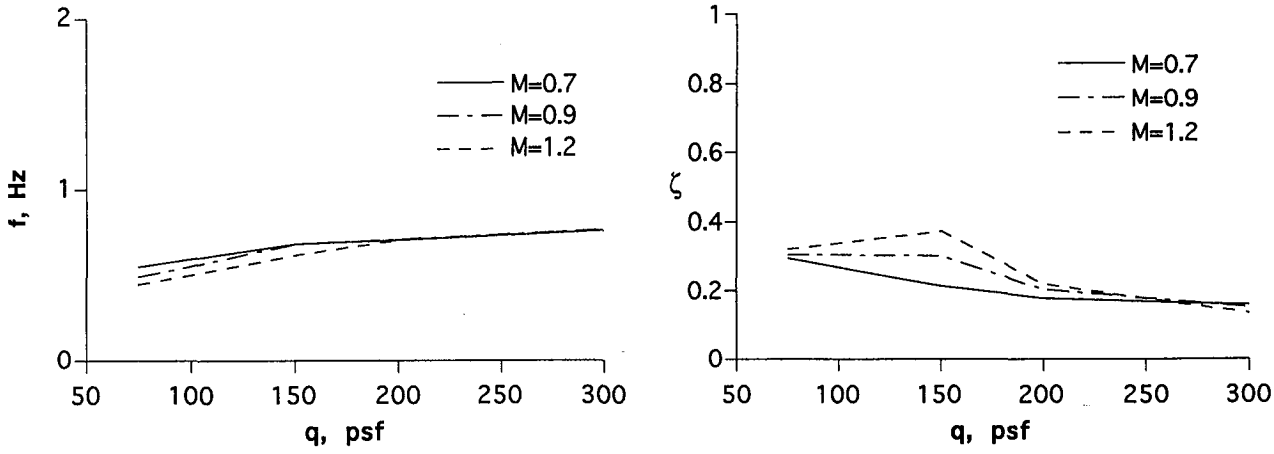

Figure 4(c) Lateral translation

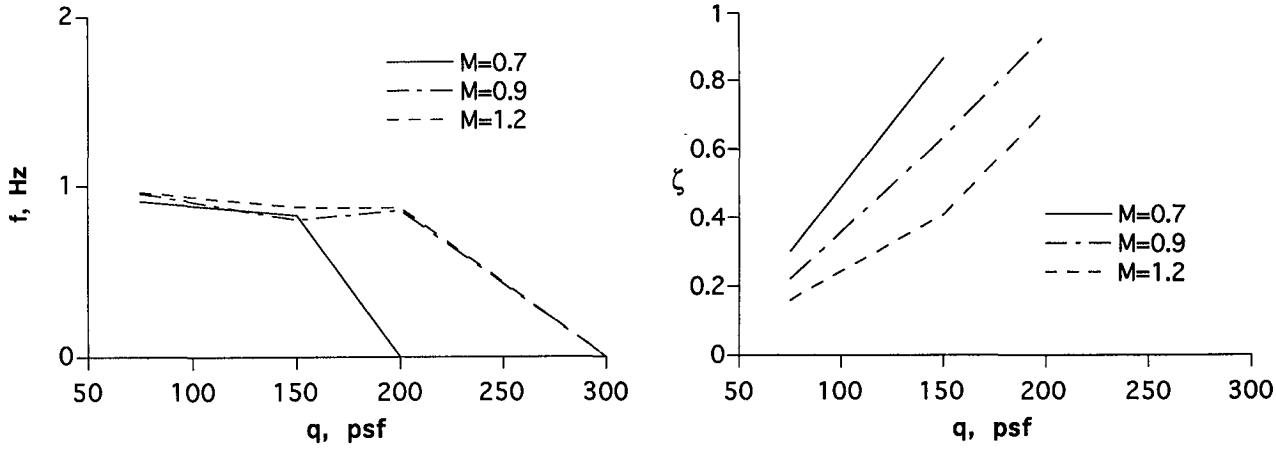

Figure 4(d) Roll-yaw

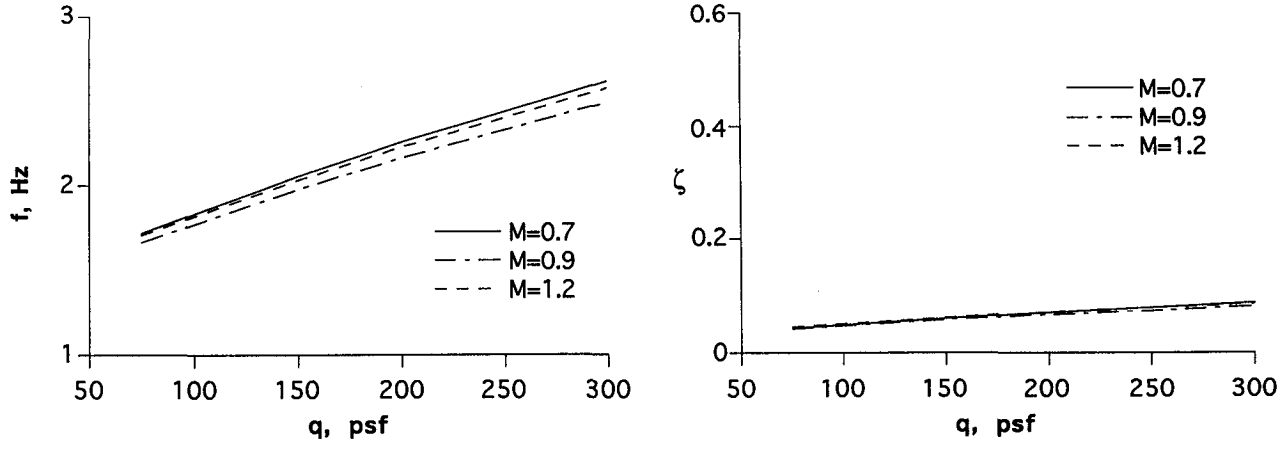

Figure 4(e) Dutch roll

Figure 4. Rigid body modes for Configuration One with respect to dynamic pressure

Cable geometry

The effect of cable geometry (cable tie-down locations on the tunnel walls) on rigid body stability was also analyzed for Configuration One. The cable pulley bracket locations in the model were determined prior to this analysis, thus the effect of varying their location on the model fuselage was not examined. Since the vertical translation mode of Configuration One for Cable Geometry 1 was unstable for most of the subsonic cases (Figures 3a and 4a), Cable Geometry 2 and Cable Geometry 3 were used to find a more stable geometry. The damping ratio of the vertical translation mode increased significantly when the rear cable was moved further aft (Cable Geometry 2). Damping was further increased when the front cable tie-down position was also moved forward (Cable Geometry 3). With Cable Geometry 3, the vertical translation mode was stable for all flow conditions analyzed. The damping ratio of the short-period mode, side translation mode, and dutch-roll mode decreased slightly with Cable Geometry 3; however, they remained stable. The damping ratio of the roll-yaw mode increased. Figure 5 compares vertical translation damping at M = 0.7 and q =150 psf for the three cable positions. Table 2 lists the roots, frequencies and damping of the vertical translation mode for each cable geometry. The cable tie-down locations for Cable Geometry 3 was selected for remaining analysis presented in this report and the wind-tunnel test.

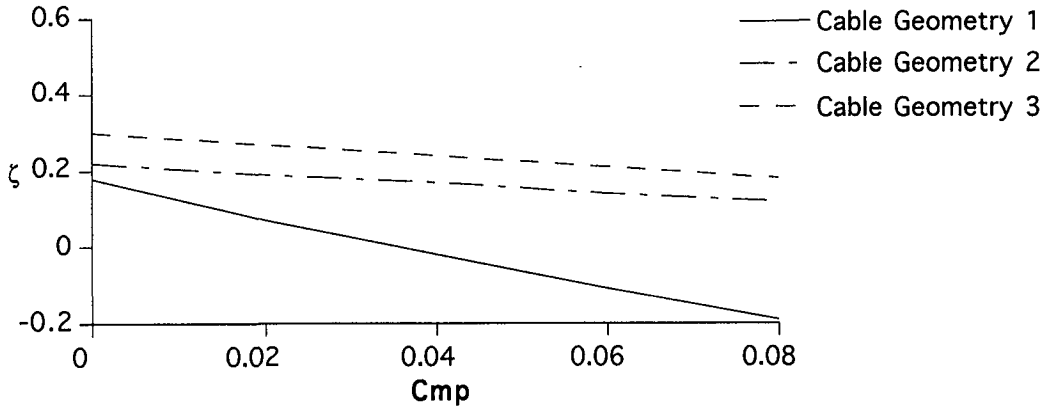

Figure 5. Effect of cable geometry on vertical translation damping of Configuration One at M = 0.7 and q =150 psf

Center of Gravity Location Effects

The effect of c.g. location on stability was examined for Configurations One and Two. The GRUMCBL input for c.g. is AERO(46) and is defined as a distance in inches from a user defined reference point. For both configurations, the reference point was at fuselage station (FS) 77. The nominal c.g. for Configuration One was 6.6 inches aft of the reference point (FS 83.6), and the nominal c.g. for Configuration Two was 10.9 inches aft of the reference point (FS 87.9). The vertical translation mode of Configuration One with its c.g. at its nominal position was stable for all Cmp values, and at all flow conditions examined. The c.g. was shifted more than 3 inches aft before Configuration One became longitudinally unstable (Figure 6a). As shown in Figure 6b, at M = 0.7 and q =150 psf, the vertical translation mode of Configuration Two, with nominal c.g. position, was unstable at higher Cmp values. Moving the c.g. forward approximately half an inch on Configuration Two stabilized vertical translation. Both configurations were unstable at approximately the same c.g. location. The calculated roots, frequencies, and damping ratios for the vertical translation mode for both configurations at M = 0.7 and q =150 psf are listed in Table 3 and Table 4.

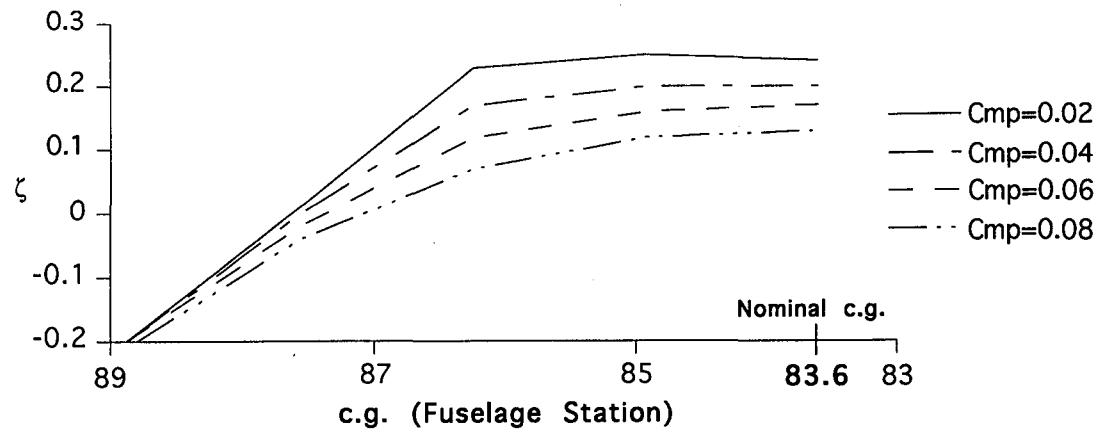

(a) Configuration One

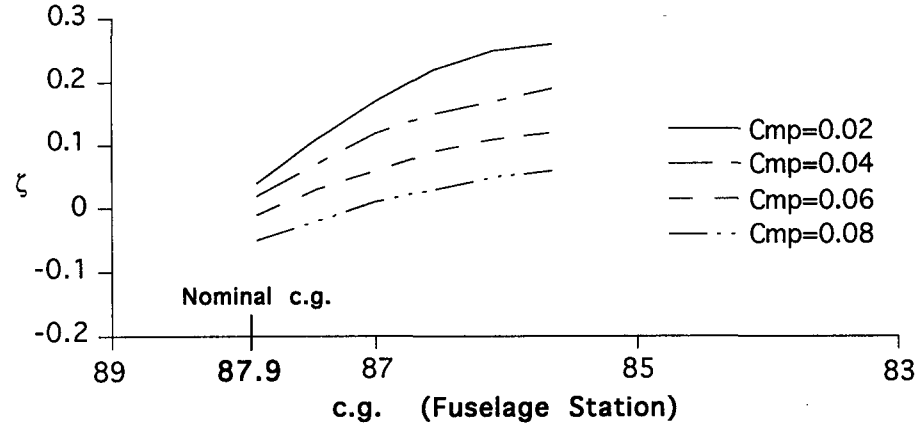

(b) Configuration Two

Figure 6. Effect of c.g. location on vertical translation damping at M = 0.7 and q = 150 psf

Rear Cable Tension Effects

The effect of rear cable tension (T_R) on stability of Configuration One was also examined. Rear cable tension (AERO(94)) values of 300 and 400 lb. were used for various flow conditions. Figures 7a through 7d show the resulting damping ratios for the vertical translation mode for four flow conditions and varied Cmp. There was a slight increase in damping as cable tension was increased at M = 0.7, however, there was an insignificant change in damping at M = 1.2.

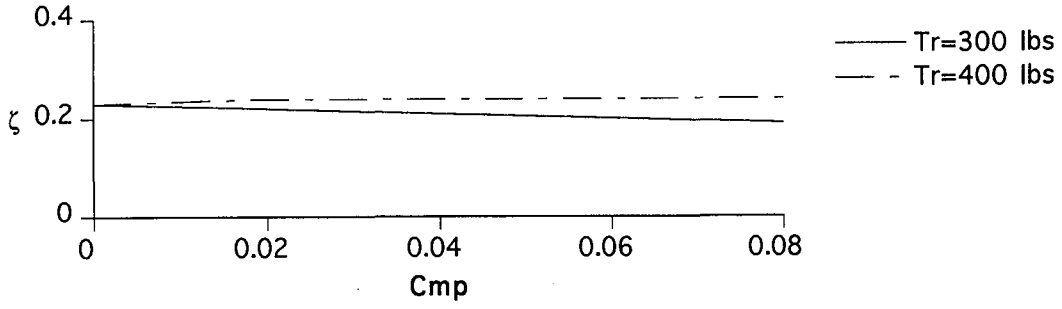

(a) M = 0.7 and q =75 psf

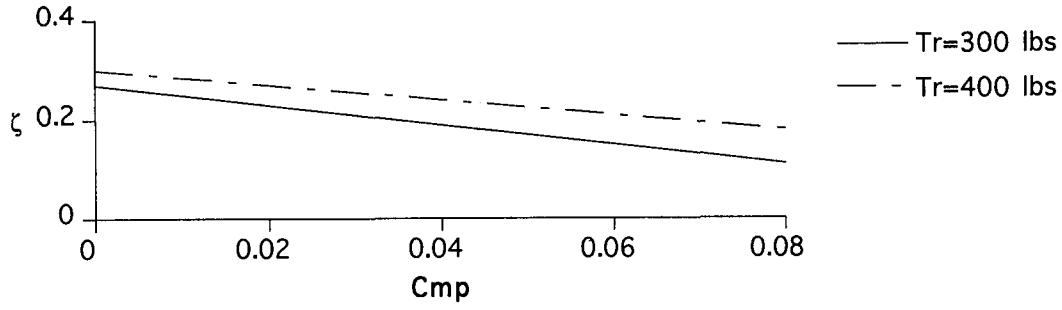

(b) M = 0.7 and q = 150 psf

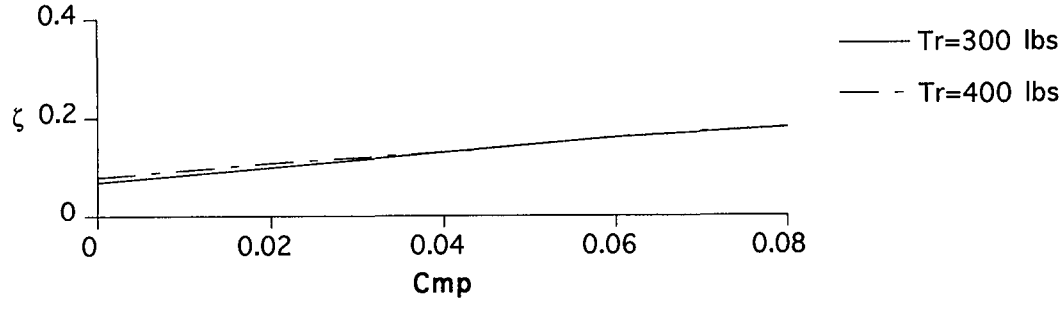

(c) M = 1.2 and q = 150 psf

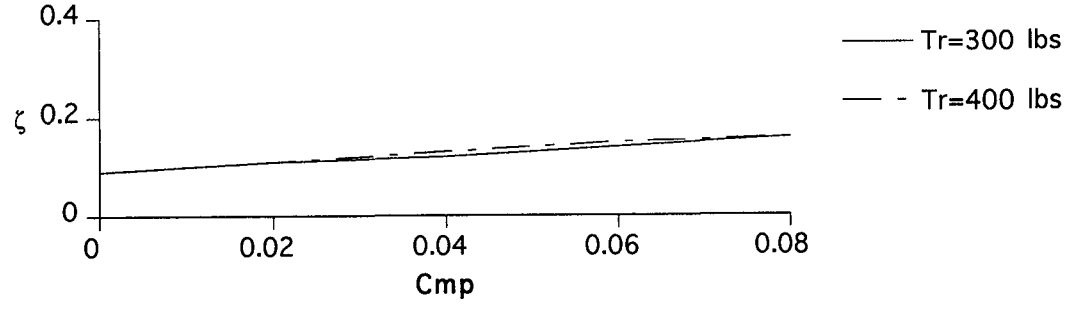

(d) M = 1.2 and q = 300 psf

Figure 7. Effect of rear cable tension on Configuration One vertical translation damping

Snubber Cable System Effects

The stability of Configuration One was examined in both the "snubbed" and "unsnubbed" condition. "Snubbed" refers to the condition when the snubber cables have been pulled taut with a remotely activated pneumatic device for the purpose of restraining the model. During the wind-tunnel test set-up, the snubber cable tension is manually set with the pneumatic device activated. During testing, tunnel speed is increased until model lift is sufficient to support the weight of the model. The pneumatic device can then be deactivated. The snubber cables become slack and no longer support the model. At this condition the model is considered unsnubbed. To calculate the effect of snubber cables on the F/A-18 E/F analytical model, the following GRUMCBL parameters were defined: upper and lower snubber cable tension, T_S, (AERO(117,118)); upper and lower snubber cable spring constant, K_S, (AERO(119,120)), and upper and lower snubber cable damping coefficient, D_S, (AERO(121,122)). Input for the upper snubber cables were identical to that of the lower snubber cables for all cases. For the snubbed condition, $T_S = 90$ lbs , $K_S = 22$ lb/in, and $D_S = 2$ lb-sec/in. From previous wind-tunnel experiments, T_S and K_S of the unsnubbed cables were found to vary with dynamic pressure such that $T_S = 1/3q$ and $K_S = .05(d_{sc}l_{sc})q$, where d_{sc} and l_{sc} are the diameter and length of the snubber cables. Also in the unsnubbed condition, snubber cable damping was found to be negligible.

Analysis of the model in the snubbed condition showed that snubbing the model increased damping of all rigid-body modes except the roll-yaw mode which decreased slightly; however, the mode remained highly damped. The snubbed and unsnubbed damping ratios for Configuration One vertical translation mode at M=0.7 and q=150 psf with varied Cmp are compared in Figure 8. The roots, frequencies, and damping ratios for all rigid-body modes, snubbed and unsnubbed, are listed in Tables 5 and 6.

The wind-tunnel wall location of the snubber cable tie-down position was also examined. It was found that moving the snubber cable tie-down point aft increased stability of the vertical translation mode. Results showing the effect of snubber cable tie-down position on stability are not shown in this report.

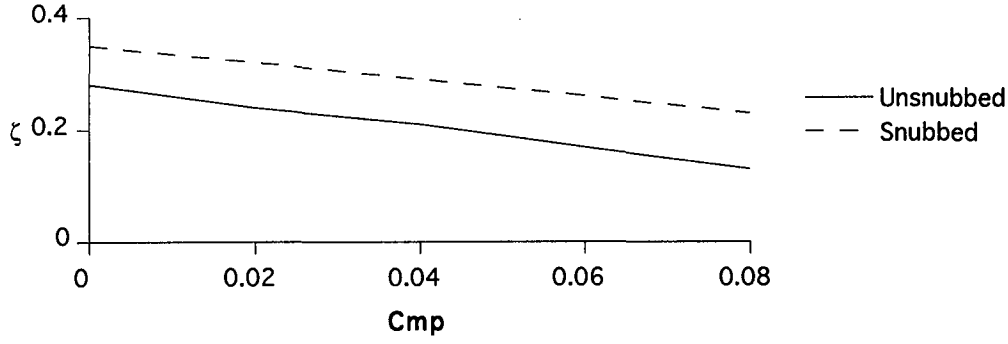

Figure 8. Configuration One vertical translation damping for "unsnubbed" and "snubbed" cases at M = 0.7 and q = 150 psf

Effects of Drag

The effects of drag on model stability were also studied analytically. A model drag coefficient (C_D) is input to GRUMCBL using AERO(14). There is a significant amount of additional drag caused by the four snubber cables which must be included in GRUMCBL analysis. The following method is an approximation used to include cable drag into the total

drag coefficient. Drag due to the model and the four snubber cables (5/32 inch diameter) is calculated by

$$Drag = \left(C_{D_M} S_M + C_{D_S} S_S\right) q$$

where C_{D_M} is the model drag coefficient, S_M is the wing area, and C_{D_S} and S_S are the effective snubber drag coefficient and snubber surface area respectively. The total drag coefficient can be calculated by

$$C_D = C_{D_M} + \frac{\left(C_{D_S} S_S\right)}{S_M}.$$

From previous wind-tunnel tests, approximate values for $\left(C_{D_S} S_S\right)$ were calculated to be one square foot at subsonic conditions, and 1.5 square feet for transonic conditions. For the F/A-18 E/F transonic model, a value of C_{D_M} =.05, and S_M =16.2 ft^2 were used which lead to a C_D of approximately 0.14.

Analysis to examine the effect of drag on stability of Configuration One and Two showed that for subsonic cases, damping of the vertical translation mode decreased as C_D increased. However, for cases above M = 1, damping of this mode increased as C_D increased.

Stability in Air

Since the initial wind-tunnel test runs were to be conducted in air with the model snubbed, stability of Configuration One with the snubber system activated was examined using velocity and flow densities appropriate for air. The damping ratios for all the rigid-body modes were lower in air than in R-12 for all flow conditions; however, all the modes were stable. The damping ratios for the vertical translation mode for air and R-12 at M=0.7 and q=150 psf with varied Cmp are compared in Figure 9.

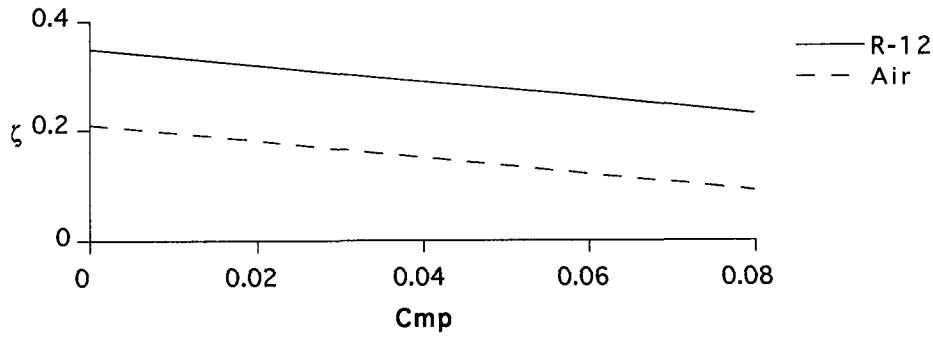

Figure 9. Configuration One vertical translation damping in R-12 and air at M = 0.7 and q = 150 psf with the snubber system activated

SUMMARY OF RESULTS

Parametric analysis of the F/A-18 E/F cable mounted model using GRUMCBL software was conducted to assess stability for TDT tests. Two configurations of the F/A-18 E/F were examined. The parameters examined were pulley-cable friction, Mach number, dynamic pressure, cable geometry, c.g. location, cable tension, snubbing the model, drag, and test medium. For the nominal cable geometry (Cable Geometry 1), Configuration One was unstable for cases with higher pulley-cable friction coefficients. A new cable geometry

(Cable Geometry 3) was determined in which Configuration One was stable for all cases evaluated. Configuration Two with the nominal c.g. position was found to be unstable for cases with higher Cmp coefficients; however, the model was stable when the c.g. was moved forward 1/2 inch. Results of this analysis show that with Cable Geometry 3, the F/A-18 E/F cable mounted models tested in the TDT should be stable provided that the c.g. is forward of fuselage station 72. The model was tested using the cable mount configuration during the first wind-tunnel entry and was stable as predicted.

REFERENCES

1. Reed, Wilmer H., III: "Aeroelasticity Matters: Some Reflections of Two Decades of Testing in the NASA Langley Research Tunnel," NASA TM-83210, 1981.

2. Reed, Wilmer H., III; and Abbott, Frank T., Jr.: "A New 'Free-Flight' Mount System for High-Speed Wind-Tunnel Flutter Models," Proceedings of Symposium on Aeroelastic & Dynamic Modeling Technology, RTD-TDR-63-4197, Pt. I, U.S. Air Force, Mar. 1964, pp.169-206.

3. Gilman, J. Jr.; and Bennett, R. M.: "A Wind-Tunnel Technique For Measuring Frequency-Response Functions For Gust Loads Analyses," J. Aircraft, vol. 3, no. 6, Nov.-Dec. 1966, pp. 535-540.

4. Redd, L. T.; Hanson, P. W.; Wynne, E. C.: "Evaluation Of A Wind-Tunnel Gust Response Technique Including Correlations With Analytical And Flight Test Results," NASA Technical Paper 1501, Nov. 1979.

5. Able, I.; "Evaluation Of A Technique For Determining Airplane Aileron Effectiveness And Roll Rate By Using An Aeroelastically Scaled Model," NASA TN D-5538, Nov. 1969.

6. Farmer, M. G.: "Flutter Studies To Determine Nacelle Aerodynamic Effects On A Fan-Jet Transport Model For Two Mount Systems And Two Wind Tunnels," NASA TN D-6003, Sept. 1970.

7. Peloubet, R. P. Jr.; Haller, R. L.; and Bolding, R. M.; "F-16 Flutter Suppression System Investigation Feasibility Study and Wind Tunnel Tests," AIAA Journal of Aircraft, February 1982.

8. Barbero, P.; and Chin, J.: User's Guide For A Computer Program To Analyze The LRC 16' Transonic Dynamics Tunnel Cable Mount System. NASA-CR-132313, 1973.

Table 1. Configuration One GRUMCBL Input Data (Cable Geometry 3)

AERO	Description	Units	M=0.5	M=1.2*	AERO	Description	Units	M=0.5	M=1.2*
1	C_{D_u}	1/ft./sec.	0.0131	0.0089	47	Distance from model mass & inertia	in.	-1.2	
2	C_{L_u}	1/ft./sec.	0.0339	0.0447		reference center to the equation			
3	C_{m_u}	1/ft./sec.	0.0164	0.0456		reference center along the z axis.			
4	C_{D_α}	1/rad	0.692	-0.0277	48	Tunnel Mach Number	N.D.	0.5	1.2
5	C_{L_α}	1/rad	4.3	4.27	49	Tunnel Velocity	ft/sec	252	606
6	C_{m_α}	1/rad	-0.407	-2.33	50	Model Mass	slugs	6.6	
7	C_{D_q}	1/rad/sec.	0		51	Tunnel Density (R-12)	slug/ft^3	0.00236	0.00123
8	C_{L_q}	1/rad/sec.	4.45	6.21	52	Model Weight	lbs	213	
9	C_{m_q}	1/rad/sec.	-5.83	-7.36	53	Model Reference Span	ft	7.53	
10	C_{D_0}	N.D.	0.14		54	Model Reference Chord	ft	2.36	
11	C_{L_0}	N.D.	-0.0204	0.0116	55	Model Reference Wing Area, (S_M)	ft^2	16.2	
12	C_{m_0}	N.D.	0.00635	0.085	56	Model Cross Product of Inertia, (I_{xz})	slug/ft^2	-0.495	
13	$C_{D_{\delta_e}}$	1/rad	0.0977	0.0565	57	Roll inertia, body axis at c.g. (I_{xx})	slug/ft^2	8.25	
14	$C_{L_{\delta_e}}$	1/rad	0.742	0.642	58	Pitch inertia, body axis at c.g. (I_{yy})	slug/ft^2	21.3	
15	$C_{m_{\delta_e}}$	1/rad	-0.975	-1.12	59	Yaw inertia, body axis at c.g. (I_{ZZ})	slug/ft^2	28.3	
16	$C_{D_{\dot{\alpha}}}$	1/rad/sec	0		68	Water line, upper rear cable tie-	in.	96	
17	$C_{L_{\dot{\alpha}}}$	1/rad/sec	2.3	1.23		down point (rear vertical)			
18	$C_{m_{\dot{\alpha}}}$	1/rad/sec	-1.03	-0.181	69	Water line, lower rear cable tie-	in.	-96	
19	C_{y_β}	1/rad/sec	-0.999	-0.961		down point (rear vertical)			
20	C_{l_β}	1/rad	-0.137	-0.178	70	Water line, horizontal front cable	in.	0	
21	C_{n_β}	1/rad	0.137	0.109		tie-down point (front horizontal)			
22	C_{y_p}	1/rad/sec	0.0285	-0.0644	72	Tunnel station, front cable tie-down	in.	516	
23	C_{l_p}	1/rad/sec	-0.394	-0.525		point (front vertical or horizontal)			
24	C_{n_p}	1/rad/sec	-0.0183	0.0254	73	Tunnel station, rear cable tie-down	in.	960	
25	C_{y_n}	1/rad/sec	0.359	0.401		point (rear vertical or horizontal)			
26	C_{l_r}	1/rad/sec	0.323	0.192	74	Butt line, horizontal front cable tie-	in.	96	
27	C_{n_r}	1/rad/sec	-0.166	-0.158		down point (front horizontal)			
28	$C_{y_{\delta_r}}$	1/rad	0.293	0.212	75	Butt line, horizontal rear cable tie-	in.	0	
29	$C_{l_{\delta_r}}$	1/rad	0.019	0.0139		down point (rear horizontal)			
30	$C_{n_{\delta_r}}$	1/rad	-0.103	-0.0849	76	Water line, equation reference point	in.	0	
31	$C_{y_{\delta_a}}$	1/rad	-0.0241	-0.0127	77	Tunnel station, equation reference pt.	in.	852	
32	$C_{l_{\delta_a}}$	1/rad	0.074	0.051	78	Butt line, equation reference point	in.	0	
33	$C_{n_{\delta_a}}$	1/rad	0.00708	0.00475	80	Distance along X axis from reference	in.	20	
34	$C_{y_{\delta_s}}$	1/rad	-0.0601	-0.0331		center to vertical rear pulley			
35	$C_{l_{\delta_s}}$	1/rad	0.0483	0.0543	81	Distance along X axis from reference	in.	22.5	
36	$C_{n_{\delta_s}}$	1/rad	0.0225	0.007		center to horizontal front pulley			
44	Distance from aerodynamic center to	in.	-6.6		85	Distance along Z axis from reference	in.	5.75	
	the eqn ref center along the x axis					center to upper rear pulley			
45	Distance from aerodynamic center to	in.	-1.2		86	Distance along Z axis from reference	in.	2	
	the eqn ref center along the z axis					center to lower rear pulley			
46	Distance from model mass & inertia	in.	-6.6		87	Distance along Y axis from reference	in.	1.5	
	reference center to the equation					center to horizontal front pulley			
	reference center along the x axis.				91	Radius of horizontal front pulley	in.	1	

Table 1. Cont'd

AERO	Description	Units	M=0.5	M=1.2*
92	Radius of vertical rear pulley	in.	1	
94	Rear cable tension, (T_R)	lbs.	300	
95	Rear cable spring constant	lbs./in.	50	
96	Pulley Coulomb friction	ft-lbs/rad	0	
104	Rear pulley friction coeff, (C_{mpr})	ft-lbs/rad/sec	0-.08	
105	Distance along X axis from model upper snubber attachment point to the equation reference center	in.	12	
106	Distance along Y axis from model upper snubber attachment point to the equation reference center	in.	9	
107	Distance along Z axis from model upper snubber attachment point to the equation reference center	in.	6.25	
108	Distance along X axis from model lower snubber attachment point to the equation reference center	in.	12	
109	Distance along Y axis from model lower snubber attachment point to the equation reference center	in.	5.75	
110	Distance along Z axis from model lower snubber attachment point to the equation reference center	in.	4.75	
111	TS, upper snub. tie-down point	in.	882	
112	WL, upper snubber tie-down point	in.	45.8	
113	BL, upper snubber tie-down point	in.	96	
114	TS, lower snub. tie-down point	in.	882	
115	WL, lower snubber tie-down point	in.	-45.8	
116	BL, lower snubber tie-down point	in.	96	
117	Upper snubber cable tension, (T_s)	lbs.	25	75
118	Lower snubber cable tension, (T_s)	lbs.	25	75
119	Upper snub. cable spring const. (K_s)	lbs./in.	0.469	1.41
120	Lower snub. cable spring const. (K_s)	lbs./in.	0.469	1.41
126	Forward pulley friction coeff, (C_{mpf})	ft-lbs/rad/sec	0-.08	

*Entry only if different from Mach .5 entry

Table 2. Configuration One Vertical Translation Mode Roots

	Front cable TS (in.)	Rear cable TS (in.)
Cable Geometry 1	588	912
Cable Geometry 2	588	960
Cable Geometry 3	516	960

Cable Geometry	Cmp	Real	± Im	Freq,Hz	Damping Ratio
1	0	-0.86	4.73	0.77	0.18
	0.02	-0.34	4.62	0.74	0.07
	0.04	0.09	4.47	0.71	-0.02
	0.06	0.46	4.29	0.69	-0.11
	0.08	0.78	4.1	0.66	-0.19
2	0	-1.13	4.97	0.81	0.22
	0.02	-0.98	4.95	0.80	0.19
	0.04	-0.84	4.92	0.79	0.17
	0.06	-0.71	4.89	0.79	0.14
	0.08	-0.58	4.85	0.78	0.12
3	0	-1.25	3.95	0.66	0.30
	0.02	-1.10	3.95	0.65	0.27
	0.04	-0.97	3.95	0.65	0.24
	0.06	-0.83	3.93	0.64	0.21
	0.08	-0.70	3.92	0.63	0.18

Table 3. Configuration One vertical translation mode roots for various c.g. locations at M=0.7 and q=150 psf (Cable Geometry 3). Nominal c.g. = FS 83.60

Cmp	c.g.	F.S.	Real	±Im	Freq,Hz	Damping Ratio
.02	-11.88	88.88	1.58	7.69	1.25	-0.20
	-10.56	87.56	-0.08	7.51	1.20	0.01
	-9.24	86.24	-1.37	5.88	0.96	0.23
	-7.92	84.92	-1.22	4.72	0.78	0.25
	-6.60	83.60	-1.03	4.12	0.68	0.24
.04	-11.88	88.88	1.51	7.37	1.20	-0.20
	-10.56	87.56	0.00	7.03	1.12	0.00
	-9.24	86.24	-0.98	5.68	0.92	0.17
	-7.92	84.92	-0.97	4.68	0.76	0.20
	-6.60	83.60	-0.85	4.10	0.67	0.20
.06	-11.88	88.88	1.47	7.04	1.15	-0.20
	-10.56	87.56	0.12	6.62	1.05	-0.02
	-9.24	86.24	-0.66	5.49	0.88	0.12
	-7.92	84.92	-0.74	4.63	0.75	0.16
	-6.60	83.60	-0.69	4.08	0.66	0.17
.08	-11.88	88.88	1.46	6.73	1.10	-0.21
	-10.56	87.56	0.27	6.27	1.00	-0.04
	-9.24	86.24	-0.40	5.32	0.85	0.07
	-7.92	84.92	-0.53	4.56	0.73	0.12
	-6.60	83.60	-0.53	4.05	0.65	0.13

Table 4. Configuration Two vertical translation mode roots for various c.g. locations at M=0.7 and q=150 psf (Cable Geometry 3). Nominal c.g. = FS 87.90

Cmp	c.g	F.S.	Real	±Im	Freq,Hz	Damping Ratio
.02	-10.90	87.90	-0.37	8.89	1.42	0.04
	-10.35	87.45	-0.91	8.57	1.37	0.11
	-9.90	87.00	-1.39	8.08	1.30	0.17
	-9.45	86.55	-1.67	7.49	1.22	0.22
	-9.00	86.10	-1.76	6.94	1.14	0.25
	-8.55	85.65	-1.75	6.48	1.07	0.26
.04	-10.90	87.90	-0.17	8.16	1.30	0.02
	-10.35	87.45	-0.56	7.83	0.00	0.07
	-9.90	87.00	-0.86	7.43	1.19	0.12
	-9.45	86.55	-1.06	7.02	1.13	0.15
	-9.00	86.10	-1.16	6.63	1.07	0.17
	-8.55	85.65	-1.20	6.28	1.02	0.19
.06	-10.90	87.90	0.09	7.56	1.20	-0.01
	-10.35	87.45	-0.20	7.28	1.16	0.03
	-9.90	87.00	-0.43	6.97	1.11	0.06
	-9.45	86.55	-0.59	6.65	1.06	0.09
	-9.00	86.10	-0.69	6.35	1.02	0.11
	-8.55	85.65	-0.75	6.07	0.97	0.12
.08	-10.90	87.90	0.36	7.08	1.13	-0.05
	-10.35	87.45	0.12	6.84	1.09	-0.02
	-9.90	87.00	-0.06	6.59	1.05	0.01
	-9.45	86.55	-0.20	6.34	1.01	0.03
	-9.00	86.10	-0.31	6.10	0.97	0.05
	-8.55	85.65	-0.38	5.87	0.94	0.06

Table 5. Configuration One Rigid-Body Modes "Unsnubbed" (Cable Geometry 3)

		M=0.7		q=75 psf		M=0.7		q=150 psf	
Mode	Cmp	Real	±Im	Freq, Hz	Damping ratio	Real	±Im	Freq, Hz	Damping ratio
Vertical Translation	0.00	-0.78	3.40	0.55	0.22	-1.17	4.00	0.66	0.28
	0.02	-0.74	3.39	0.55	0.21	-1.00	4.00	0.66	0.24
	0.04	-0.71	3.38	0.55	0.21	-0.84	3.98	0.65	0.21
	0.06	-0.68	3.37	0.55	0.20	-0.68	3.96	0.64	0.17
	0.08	-0.65	3.36	0.54	0.19	-0.53	3.94	0.63	0.13
Short Period	0.00	-2.50	12.98	2.10	0.19	-5.37	15.49	2.61	0.33
	0.02	-2.78	12.98	2.11	0.21	-5.81	15.53	2.64	0.35
	0.04	-3.06	12.97	2.12	0.23	-6.23	15.58	2.67	0.37
	0.06	-3.34	12.96	2.13	0.25	-6.65	15.63	2.70	0.39
	0.08	-3.62	12.95	2.14	0.27	-7.06	15.68	2.74	0.41
Lateral Translation	0.00	-0.43	4.04	0.65	0.11	-0.38	4.73	0.76	0.08
	0.02	-0.56	4.09	0.66	0.14	-0.46	4.76	0.76	0.10
	0.04	-0.70	4.16	0.67	0.17	-0.55	4.79	0.77	0.11
	0.06	-0.87	4.26	0.69	0.20	-0.64	4.82	0.77	0.13
	0.08	-1.06	4.43	0.72	0.23	-0.73	4.85	0.78	0.15
Roll-yaw	0.00	-2.17	4.68	0.82	0.42	-4.84	3.94	0.99	0.78
	0.02	-2.10	4.62	0.81	0.41	-4.82	3.90	0.99	0.78
	0.04	-2.01	4.54	0.79	0.40	-4.79	3.86	0.98	0.78
	0.06	-1.89	4.44	0.77	0.39	-4.77	3.82	0.97	0.78
	0.08	-1.75	4.26	0.73	0.38	-4.74	3.77	0.96	0.78
Dutch roll	0.00	-0.41	11.21	1.79	0.04	-0.75	13.47	2.15	0.06
	0.02	-0.42	11.20	1.78	0.04	-0.76	13.46	2.15	0.06
	0.04	-0.43	11.20	1.78	0.04	-0.76	13.45	2.15	0.06
	0.06	-0.45	11.19	1.78	0.04	-0.76	13.45	2.14	0.06
	0.08	-0.46	11.18	1.78	0.04	-0.76	13.44	2.14	0.06
		M=1.2		q=150 psf		M=1.2		q=300 psf	
Mode	Cmp	Real	±Im	Freq, Hz	Damping ratio	Real	±Im	Freq, Hz	Damping ratio
Vertical Translation	0.00	-0.25	3.94	0.63	0.06	-0.38	5.02	0.80	0.08
	0.02	-0.34	3.93	0.63	0.09	-0.45	5.01	0.80	0.09
	0.04	-0.44	3.92	0.63	0.11	-0.52	5.00	0.80	0.10
	0.06	-0.53	3.91	0.63	0.13	-0.60	4.99	0.80	0.12
	0.08	-0.62	3.89	0.63	0.16	-0.67	4.98	0.80	0.13
Short Period	0.00	-3.52	27.34	4.39	0.13	-7.15	37.49	6.08	0.19
	0.02	-3.70	27.33	4.39	0.13	-7.36	37.48	6.08	0.19
	0.04	-3.88	27.31	4.39	0.14	-7.56	37.46	6.08	0.20
	0.06	-4.06	27.29	4.39	0.15	-7.77	37.44	6.09	0.20
	0.08	-4.24	27.27	4.39	0.15	-7.98	37.42	6.09	0.21
Lateral Translation	0.00	-0.41	4.64	0.74	0.09	-0.37	5.86	0.93	0.06
	0.02	-0.53	4.68	0.75	0.11	-0.46	5.87	0.94	0.08
	0.04	-0.66	4.73	0.76	0.14	-0.55	5.89	0.94	0.09
	0.06	-0.79	4.78	0.77	0.16	-0.64	5.91	0.95	0.11
	0.08	-0.94	4.84	0.78	0.19	-0.73	5.93	0.95	0.12
Roll-yaw	0.00	-3.16	5.53	1.01	0.50	-6.85	4.75	1.33	0.82
	0.02	-3.10	5.49	1.00	0.49	-6.83	4.73	1.32	0.82
	0.04	-3.03	5.44	0.99	0.49	-6.80	4.71	1.32	0.82
	0.06	-2.94	5.38	0.98	0.48	-6.78	4.69	1.31	0.82
	0.08	-2.85	5.32	0.96	0.47	-6.76	4.67	1.31	0.82
Dutch roll	0.00	-0.74	13.35	2.13	0.06	-1.37	16.90	2.70	0.08
	0.02	-0.75	13.34	2.13	0.06	-1.36	16.89	2.70	0.08
	0.04	-0.76	13.34	2.13	0.06	-1.36	16.88	2.70	0.08
	0.06	-0.77	13.33	2.12	0.06	-1.36	16.88	2.69	0.08
	0.08	-0.78	13.32	2.12	0.06	-1.35	16.87	2.69	0.08

Table 6. Configuration One Rigid-Body Modes "Snubbed" (Cable Geometry 3)

		M=0.7		q=75 psf		M=0.7		q=150 psf	
Mode	Cmp	Real	±Im	Freq, Hz	Damping ratio	Real	±Im	Freq, Hz	Damping ratio
Vertical Translation	0.00	-1.53	4.97	0.83	0.29	-1.84	4.98	0.85	0.35
	0.02	-1.49	4.97	0.83	0.29	-1.67	4.99	0.84	0.32
	0.04	-1.46	4.97	0.82	0.28	-1.50	4.99	0.83	0.29
	0.06	-1.42	4.97	0.82	0.27	-1.34	4.97	0.82	0.26
	0.08	-1.38	4.97	0.82	0.27	-1.19	4.96	0.81	0.23
Short Period	0.00	-2.97	13.85	2.26	0.21	-5.93	16.08	2.73	0.35
	0.02	-3.26	13.82	2.26	0.23	-6.36	16.09	2.75	0.37
	0.04	-3.54	13.78	2.26	0.25	-6.79	16.11	2.78	0.39
	0.06	-3.83	13.73	2.27	0.27	-7.21	16.13	2.81	0.41
	0.08	-4.11	13.69	2.28	0.29	-7.62	16.15	2.84	0.43
Lateral Translation	0.00	-2.21	6.46	1.09	0.32	-4.65	5.35	1.13	0.66
	0.02	-2.23	6.45	1.09	0.33	-4.66	5.34	1.13	0.66
	0.04	-2.25	6.44	1.09	0.33	-4.67	5.32	1.13	0.66
	0.06	-2.26	6.43	1.08	0.33	-4.68	5.30	1.13	0.66
	0.08	-2.28	6.42	1.08	0.34	-4.69	5.28	1.12	0.66
Roll-yaw	0.00	-6.04	13.37	2.34	0.41	-5.83	12.77	2.24	0.42
	0.02	-6.06	13.35	2.33	0.41	-5.87	12.73	2.23	0.42
	0.04	-6.08	13.33	2.33	0.42	-5.90	12.69	2.23	0.42
	0.06	-6.11	13.31	2.33	0.42	-5.94	12.65	2.22	0.43
	0.08	-6.13	13.28	2.33	0.42	-5.98	12.61	2.22	0.43
Dutch roll	0.00	-0.71	11.40	1.82	0.06	-1.43	13.56	2.17	0.10
	0.02	-0.74	11.42	1.82	0.06	-1.45	13.59	2.18	0.11
	0.04	-0.76	11.43	1.82	0.07	-1.47	13.63	2.18	0.11
	0.06	-0.79	11.44	1.83	0.07	-1.49	13.66	2.19	0.11
	0.08	-0.81	11.45	1.83	0.07	-1.51	13.70	2.19	0.11
		M=1.2		q=150 psf		M=1.2		q=300 psf	
Mode	Cmp	Real	±Im	Freq, Hz	Damping ratio	Real	±Im	Freq, Hz	Damping ratio
Vertical Translation	0.00	-1.24	6.19	1.01	0.20	-1.33	6.58	1.07	0.20
	0.02	-1.32	6.18	1.01	0.21	-1.40	6.56	1.07	0.21
	0.04	-1.41	6.16	1.01	0.22	-1.47	6.54	1.07	0.22
	0.06	-1.50	6.14	1.01	0.24	-1.54	6.52	1.07	0.23
	0.08	-1.59	6.12	1.01	0.25	-1.61	6.50	1.07	0.24
Short Period	0.00	-3.76	27.43	4.41	0.14	-7.43	37.38	6.07	0.19
	0.02	-3.95	27.41	4.41	0.14	-7.64	37.36	6.07	0.20
	0.04	-4.13	27.37	4.41	0.15	-7.85	37.33	6.07	0.21
	0.06	-4.31	27.34	4.41	0.16	-8.06	37.30	6.07	0.21
	0.08	-4.50	27.30	4.40	0.16	-8.27	37.26	6.08	0.22
Lateral Translation	0.00	-3.14	6.17	1.10	0.45	-6.49	4.11	1.22	0.84
	0.02	-3.16	6.16	1.10	0.46	-6.49	4.09	1.22	0.85
	0.04	-3.18	6.15	1.10	0.46	-6.49	4.07	1.22	0.85
	0.06	-3.20	6.13	1.10	0.46	-6.49	4.05	1.22	0.85
	0.08	-3.22	6.12	1.10	0.47	-6.49	4.03	1.22	0.85
Roll-yaw	0.00	-5.67	13.21	2.29	0.39	-6.22	12.06	2.16	0.46
	0.02	-5.70	13.18	2.29	0.40	-6.29	12.02	2.16	0.46
	0.04	-5.72	13.14	2.28	0.40	-6.35	11.99	2.16	0.47
	0.06	-5.74	13.11	2.28	0.40	-6.42	11.96	2.16	0.47
	0.08	-5.77	13.08	2.28	0.40	-6.48	11.92	2.16	0.48
Dutch roll	0.00	-1.43	13.47	2.16	0.11	-1.80	17.26	2.76	0.10
	0.02	-1.45	13.49	2.16	0.11	-1.80	17.29	2.77	0.10
	0.04	-1.47	13.52	2.16	0.11	-1.80	17.32	2.77	0.10
	0.06	-1.49	13.54	2.17	0.11	-1.80	17.35	2.78	0.10
	0.08	-1.52	13.57	2.17	0.11	-1.81	17.37	2.78	0.10

Appendix
GRUMCBL output listing example

1 CASE NO=801 CMP=0.04 - Config 5 - M=0.90 - q=75 FRONT CABLE HORIZONTAL,
REAR CABLE VERTICAL, NO SNUBBERS

CODE NOS. FOR THIS CASE.

1	2	3	4	5	6	7	8	9	10	11	12	13	14	15	16	17	18	19	20	21	22	23	24
80	1	0	0	0	2	0	4	3	0	0	0	0	0	0	0	0	0	0	0	0	0	0	0

INPUT DATA AS SPECIFIED IN AERO ARRAY

AERO(1)= .217	AERO(2)= .199	AERO(3)= .159	AERO(4)= .0563	AERO(5)= 5.00
AERO(6)= -.927	AERO(7)= .000	AERO(8)= 6.06	AERO(9)= -8.22	AERO(10)= .140
AERO(11)= -.0234	AERO(12)= .0787	AERO(13)= .0780	AERO(14)= .882	AERO(15)= -1.32
AERO(16)= .000	AERO(17)= 2.31	AERO(18)= -2.35	AERO(19)= -.939	AERO(20)= -.146
AERO(21)= .0969	AERO(22)= -.011	AERO(23)= -.463	AERO(24)= .0140	AERO(25)= .346
AERO(26)= .199	AERO(27)= -.107	AERO(28)= .290	AERO(29)= .0228	AERO(30)= -.110
AERO(31)= -.0277	AERO(32)= .0715	AERO(33)= .0074	AERO(34)= -.0440	AERO(35)= .047
AERO(36)= .0146	AERO(37)= .000	AERO(38)= .000	AERO(39)= .000	AERO(40)= .000
AERO(41)= .000	AERO(42)= .000	AERO(43)= .000	AERO(44)= -6.60	AERO(45)= -1.20
AERO(46)= -6.60	AERO(47)= -1.20	AERO(48)= .900	AERO(49)= 454.	AERO(50)= 6.60
AERO(51)= .0007	AERO(52)= 213.	AERO(53)= 7.53	AERO(54)= 2.36	AERO(55)= 16.2
AERO(56)= -.495	AERO(57)= 8.25	AERO(58)= 21.3	AERO(59)= 28.3	AERO(60)= .000
AERO(61)= .000	AERO(62)= .000	AERO(63)= .000	AERO(64)= .000	AERO(65)= .000
AERO(66)= .000	AERO(67)= .000	AERO(68)= 96.0	AERO(69)= -96.0	AERO(70)= .000
AERO(71)= .000	AERO(72)= 588.	AERO(73)= 912.	AERO(74)= 96.0	AERO(75)= .000
AERO(76)= .000	AERO(77)= 852.	AERO(78)= .000	AERO(79)= .000	AERO(80)= 20.0
AERO(81)= 22.5	AERO(82)= .000	AERO(83)= .000	AERO(84)= .000	AERO(85)= 5.75
AERO(86)= 2.00	AERO(87)= 1.50	AERO(88)= .000	AERO(89)= .000	AERO(90)= .000
AERO(91)= 1.00	AERO(92)= 1.00	AERO(93)= .000	AERO(94)= 400.	AERO(95)= 50.0
AERO(96)= .000	AERO(97)= .000	AERO(98)= .000	AERO(99)= .000	AERO(100)= .000
AERO(101)= .000	AERO(102)= .000	AERO(103)= .000	AERO(104)= .040	AERO(105)= 12.0
AERO(106)= 9.00	AERO(107)= 6.25	AERO(108)= 12.0	AERO(109)= 5.75	AERO(110)= 4.75
AERO(111)= 888.	AERO(112)= 45.8	AERO(113)= 96.0	AERO(114)= 888.	AERO(115)= -45.8
AERO(116)= 96.0	AERO(117)= 80.0	AERO(118)= 80.0	AERO(119)= 1.13	AERO(120)= 1.13
AERO(121)= .000	AERO(122)= .000	AERO(123)= .000	AERO(124)= .000	AERO(125)= .000
AERO(126)= .040	AERO(127)= .000	AERO(128)= .000	AERO(129)= .000	AERO(130)= .000
AERO(131)= .000	AERO(132)= .000	AERO(133)= .000	AERO(134)= .000	AERO(135)= .000
AERO(136)= .000	AERO(137)= .000	AERO(138)= .000	AERO(139)= .000	AERO(140)= .000
AERO(141)= .000	AERO(142)= .000	AERO(143)= .000	AERO(144)= .000	AERO(145)= .000
AERO(146)= .000	AERO(147)= .000	AERO(148)= .000	AERO(149)= .000	AERO(150)= .000
AERO(151)= .000	AERO(152)= .000	AERO(153)= .000	AERO(154)= .000	AERO(155)= .000
AERO(156)= .000	AERO(157)= .000	AERO(158)= .000	AERO(159)= .000	AERO(160)= .000

VEH. ATT.,DEFLTN,+ CABLE TENSION
THETA = 1.97 DEG
DELTA = 2.52 DEG
FRT CAB. TENSION= .282981E+03 LBS
RR CAB. TENSION = .397899E+03 LBS

++++ LONGITUDINAL STABILITY ++++
POLYNOMIAL W CONST TERM FIRST

-6.83E+05 -3.52E+04 -6.26E+04 -2.14E+03 -2.62E+02

REAL	IMAGINARY	T H/D-SEC	1/T H/D	PERIOD-SEC	DNATF-CPS	UNDNAT-CPS	DAMP RATIO	DECAY RATIO
-9.43E-02	+ -.3397E+01	7.35E+00	1.36E-01	1.85E+00	5.41E-01	5.41E-01	2.78E-02	8.40E-01
-3.99E+00	+ -.1450E+02	1.74E-01	5.75E+00	4.33E-01	2.31E+00	2.39E+00	2.65E-01	1.78E-01

++++ LATERAL/DIRECTIONAL STABILITY ++++
POLYNOMIAL W CONST TERM FIRST

5.92E+07 1.64E+07 9.25E+06 9.82E+05 2.52E+05
8.37E+03 1.54E+03

REAL	IMAGINARY	T H/D-SEC	1/T H/D	PERIOD-SEC	DNATF-CPS	UNDNAT-CPS	DAMP RATIO	DECAY RATIO
-.9495E+00	+ -.2963E+01	.7300E+00	.1370E+01	.2120E+01	.4716E+00	.4953E+00	.3051E+00	.1335E+00
-.1339E+01	+ -.5888E+01	.5178E+00	.1931E+01	.1067E+01	.9371E+00	.9610E+00	.2217E+00	.2397E+00
-.4370E+00	+ -.1044E+02	.1586E+0	.6305E+00	.6021E+00	.1661E+01	.1662E+01	.4184E-01	.7686E+00

REPORT DOCUMENTATION PAGE

Form Approved
OMB No. 0704-0188

1. AGENCY USE ONLY (*Leave blank*)	2. REPORT DATE	3. REPORT TYPE AND DATES COVERED
	June 1994	Technical Memorandum

4. TITLE AND SUBTITLE
A Stability Analysis of an F/A-18 E/F Cable Mount Model

5. FUNDING NUMBERS
WU 505-63-50-13

6. AUTHOR(S)
Nancy Thompson and Moses Farmer

7. PERFORMING ORGANIZATION NAME(S) AND ADDRESS(ES)
NASA Langley Research Center
Hampton, VA 23665-5225

8. PERFORMING ORGANIZATION REPORT NUMBER

9. SPONSORING / MONITORING AGENCY NAME(S) AND ADDRESS(ES)
National Aeronautics and Space Administration
Washington, DC 20546-0001

10. SPONSORING / MONITORING AGENCY REPORT NUMBER
NASA TM-108989

11. SUPPLEMENTARY NOTES

12a. DISTRIBUTION / AVAILABILITY STATEMENT
Unclassified-Unlimited
Subject Category 05

12b. DISTRIBUTION CODE

13. ABSTRACT (*Maximum 200 words*)

A full-span F/A-18 E/F cable mounted wind-tunnel model is part of a flutter clearance program at the NASA Langley Transonic Dynamics Tunnel. Parametric analysis of this model using GRUMCBL software was conducted to asses stability for wind-tunnel tests. Two configurations of the F/A-18 E/F were examined. The parameters examined were pulley-cable friction, mach number, dynamic pressure, cable geometry, center of gravity location, cable tension, snubbing the model, drag, and test medium. For the nominal cable geometry (Cable Geometry 1), Configuration One was unstable for cases with higher pulley-cable friction coefficients. A new cable geometry (Cable Geometry 3) was determined in which Configuration One was stable for all cases evaluated. Configuration Two with the nominal center of gravity position was found to be unstable for cases with higher pulley-cable friction coefficients; however, the model was stable when the center of gravity moved forward 1/2 . The model was tested using the cable mount system during the initial wind-tunnel entry and was stable as predicted

14. SUBJECT TERMS
rigid body stability analysis
cable-mounted wind-tunnel model

15. NUMBER OF PAGES
23

16. PRICE CODE
A03

17. SECURITY CLASSIFICATION OF REPORT	18. SECURITY CLASSIFICATION OF THIS PAGE	19. SECURITY CLASSIFICATION OF ABSTRACT	20. LIMITATION OF ABSTRACT
Unclassified	Unclassified		